FUNCTION™ american physiological society

FUNCTION, 2024, 5(2): zqae003

https://doi.org/10.1093/function/zqae003
Advance Access Publication Date: 19 January 2024
Original Research

RESEARCH ARTICLE

Phosphodiesterases Mediate the Augmentation of Myogenic Constriction by Inhibitory G Protein Signaling and is Negatively Modulated by the Dual Action of RGS2 and 5

Bo Sun, Nia Smith, Alethia J. Dixon, Patrick Osei-Owusu*

Department of Physiology and Biophysics, Case Western Reserve University School of Medicine, Cleveland, OH 44106, USA

*Address correspondence to P.O-O. (e-mail: pxo70@case.edu)

Abstract

G protein regulation by regulators of G protein signaling (RGS) proteins play a key role in vascular tone maintenance. The loss of $G_{i/o}$ and $G_{q/11}$ regulation by RGS2 and RGS5 in non-pregnant mice is implicated in augmented vascular tone and decreased uterine blood flow (UBF). RGS2 and 5 are closely related and co-expressed in uterine arteries (UA). However, whether and how RGS2 and 5 coordinate their regulatory activities to finetune G protein signaling and regulate vascular tone are unclear. Here, we determined how the integrated activity of RGS2 and 5 modulates vascular tone to promote UBF. Using ultrasonography and pressure myography, we examined uterine hemodynamics and myogenic tone (MT) of UA of wild type (WT), *Rgs2*$^{-/-}$, *Rgs5*$^{-/-}$, and *Rgs2/5* dbKO mice. We found that MT was reduced in *Rgs5*$^{-/-}$ relative to WT or *Rgs2*$^{-/-}$ UA. Activating $G_{i/o}$ with dopamine increased, whereas exogenous cAMP decreased MT in *Rgs5*$^{-/-}$ UA to levels in WT UA. Dual deletion of *Rgs2* and 5 abolished the reduced MT due to the absence of *Rgs5* and enhanced dopamine-induced $G_{i/o}$ effects in *Rgs2/5* dbKO UA. Conversely, and as in WT UA, $G_{i/o}$ inhibition with pertussis toxin or exogenous cAMP decreased MT in *Rgs2/5* dbKO to levels in *Rgs5*$^{-/-}$ UA. Inhibition of phosphodiesterases (PDE) concentration-dependently decreased and normalized MT in all genotypes, and blocked dopamine-induced MT augmentation in *Rgs2*$^{-/-}$, *Rgs5*$^{-/-}$, and *Rgs2/5* dbKO UA. We conclude that $G_{i/o}$ augments UA MT in the absence of RGS2 by a novel mechanism involving PDE-mediated inhibition of cAMP-dependent vasodilatation..

Submitted: 6 November 2023; **Revised:** 9 January 2024; **Accepted:** 16 January 2024

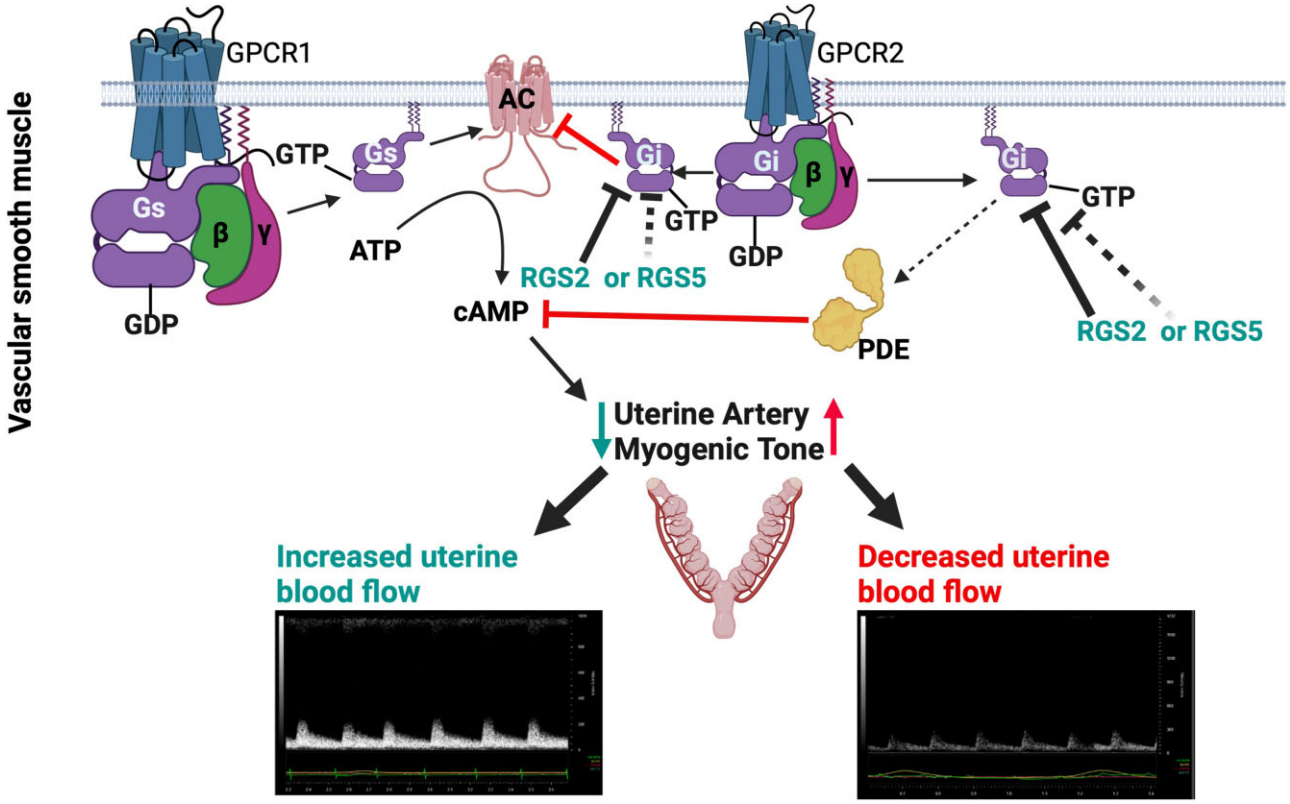

Key words: uterine hemodynamics; G protein signaling; RGS proteins; myogenic response; cAMP

Introduction

Uterine artery hemodynamics controls perfusion of the female reproductive system and can be abnormally altered in hypertensive diseases and other cardiovascular disorders. Abnormal uterine blood flow (UBF) is a hallmark of hypertensive disorders of pregnancy, including chronic hypertension, preeclampsia, and gestational hypertension with or without superimposed preeclampsia.[1–4] Abnormal UBF is also associated with low fertility rate and low gravidity and parity.[5–8] However, the mechanisms that govern the regulation of uterine artery hemodynamics and thus UBF, both in nonpregnant and pregnant states, are poorly understood. The uterine vasculature is considered a vascular bed of low impedance, characterized by high resistivity with almost negligible capacitance or compliance behavior.[6,9] The "low impedance" reflects the relationship between the low frequency of blood pressure pulsatility and the rate of vasomotion, driven largely by the biomechanical properties of the uterine vascular bed, while the "high resistivity" reflects the relatively small diameters of the arteries in the uterine vascular bed that are further reduced by the relatively high vascular tone driven mostly by myogenic reactivity to intraluminal pressure.[10,11] The uterine artery and arterial branches in the uterine vascular bed are muscular and are considered resistance arteries that readily generate myogenic response to changes in intraluminal pressure. As such, perfusion in this vascular bed is regulated largely by the vascular resistance that, in turn, is determined by vascular tone.[12] Principally, the level of tone in a resistance vascular bed is the balance between the vasodilation elicited by factors extrinsic to the vascular smooth muscle, including nitric oxide (NO) and endothelium-derived hyperpolarization factors (EDHF), vasoconstriction resulting from vascular reactivity to contractile ligands and myogenic response, a vascular smooth muscle-intrinsic property enabling small-diameter arteries and arterioles to constrict in reaction to wall stretch by increases in intraluminal pressure driving blood flow down the arterial tree.[13–18] Myogenic response depends on mechanosensing and subsequent mechanotransduction. The specific mechanosensors detecting wall stretch in the uterine vascular bed are ill-defined. However, the downstream mechanotransduction, culminating in cytoplasmic rise in calcium concentration for the activation of the contractile machinery triggering actomyosin cross-bridging and smooth muscle contraction, is relatively well established.[17–19] Nonetheless, it remains unclear how these downstream signaling pathways are regulated in the uterine vasculature to promote UBF as needed or become defective leading to reduced uterine perfusion in disease states.

Previous work by us and others has shown that the regulation of signaling via heterotrimeric G proteins of the $G_{q/11}$ and $G_{i/o}$ classes are involved in the control of uterine artery myogenic response and thus UBF in nonpregnant mice.[20,21] Several putative mechanosensing G protein-coupled receptors (GPCRs), including the angiotensin type 1a receptor and adhesion GPCRs, are proposed to couple to and activate $G_{q/11}$ G protein class in a ligand-independent manner to mediate a myogenic response.[22–25] Once activated, $G_{q/11}$ signaling triggers intracellular Ca^{2+} transients by stimulating IP_3-mediated Ca^{2+} release from internal stores via the activation of phospholipase C (PLC) that, in turn, hydrolyzes phosphatidylinositol 4,5-bisphosphate (PIP_2) to diacyl glycerol (DAG) and inositol 1,4,5 trisphosphate (IP_3).[17,22,23] Besides $G_{q/11}$, $G_{i/o}$ signaling has

also been shown to upregulate myogenic tone.[21] However, in contrast to $G_{q/11}$-mediated signaling, the mechanisms by which $G_{i/o}$ is involved in the induction and/or regulation of myogenic response involves the regulation of cyclic adenosine 3′,5′-monophosphate (cAMP) generation and signaling causing vasodilation to oppose Ca^{2+}-dependent constriction.[26–28] The activity of both $G_{q/11}$ and $G_{i/o}$ classes is finetuned by regulators of G protein signaling (RGS) proteins, which act as GTPase-activating proteins (GAPs), accelerating GTP hydrolysis via the intrinsic GTPase activity of the heterotrimeric G protein α-subunit.[29–31] The finetuning by RGS proteins is crucial to modulating myogenic tone in uterine arteries (UA). Increased $G_{i/o}$ activity, as occurs in the absence of RGS2, augments uterine artery myogenic tone and impedance to UBF in nonpregnant mice.[21] Additionally, global *Rgs2* deletion has been shown to elevate blood pressure in mice.[32] The absence of RGS5, which is closely related to RGS2 in structure and function,[29,31,33,34] has also been demonstrated to increase uterine artery reactivity to contractile agonists that activate $G_{q/11}$-coupled GPCRs,[20] while pregnant *Rgs5* null mice are reported to show gestational hypertension and preeclampsia-like features.[20,35] Together, these lines of evidence indicate that G protein regulation by both RGS2 and 5 is critical to maintaining normal UBF. The uterine vascular bed expresses multiple RGS proteins, including RGS2, 4, and 5,[35] all of which belong to the R4/B RGS family and act as GAP toward $G_{q/11}$ and $G_{i/o}$.[31,36,37] However, whether and how the activity of multiple RGS proteins is coordinated to finetune G protein activity to modulate myogenic tone, and thus UBF, is unclear.

In this study, we determined how RGS2 and 5 independently regulate $G_{i/o}$, and how their regulatory roles are integrated to modulate uterine artery myogenic tone and uterine artery hemodynamics in nonpregnant mice. Our findings reveal a novel mechanism by which $G_{i/o}$ acts to upregulate uterine artery myogenic tone. We also report that RGS2 and 5 have opposing effects on uterine artery myogenic tone, which hinge on the efficiency of regulating the inhibitory effect of $G_{i/o}$, on cAMP signaling partly via the canonical inhibition of adenylyl cyclase (AC) and a novel mechanism involving the upregulation of phosphodiesterase (PDE) activity in UA.

Materials and Methods

Animals

Female mice between the ages of 8 and 20 wk were used for all experiments. All genotypes used in the study, including wild type (WT), *Rgs2* knockout (*Rgs2*$^{-/-}$), *Rgs5* knockout (*Rgs5*$^{-/-}$), and *Rgs2/5* double knockout (*Rgs2/5* dbKO) mice, were backcrossed extensively into the Charles River C57BL/6 genetic background. The generation of *Rgs2*$^{-/-}$ and *Rgs5*$^{-/-}$ mice has been described previously.[38,39] *Rgs2/5* dbKO mice were generated from crosses between *Rgs2*$^{-/-}$ and *Rgs5*$^{-/-}$ mice, as previously described.[40] All experiments were performed in accordance with the protocols approved by the Institutional Animal Care and Use Committee at Case Western Reserve University School of Medicine, in accordance with the National Institutes of Health Guidance for the Care and Use of Laboratory Animals.

Uterine Hemodynamics Evaluation By Doppler Ultrasound

We followed the mouse Doppler ultrasound (US) protocol previously described by us and others.[21,35,41] Briefly, adult nonpregnant female mice were shaved from the mid to lower abdomen followed by the application of a depilatory agent under isoflurane anesthesia, 1 d before the US. On the day of the US, the mice were positioned on the heated platform of a Vevo 3100 Imaging Station (VisualSonics Inc., Toronto, Canada) and secured with an adhesive tape, as previously described.[21] Body temperature was maintained at 37°C throughout the animal preparation and data acquisition period with a continuous monitoring of heart and respiratory rates. Uterine arteries near the bladder were located by color Doppler using a 400-MHz probe placed over the lower abdomen, which was covered with copious amount of warm coupling gel, as previously described.[21] Few seconds of cines of the pulsed waveforms of blood flow were recorded at an insonation angle of ∼30° and a frequency of 24 Hz. Waveform recordings were taken from both the right and left UA. After baseline data acquisition, each animal received a bolus intraperitoneal injection of L-N^G-Nitroarginine methyl ester (L-NAME, 60 mg kg^{-1}, i.p.). Ten minutes later, the pulsed waveform recordings were repeated. The mice were returned to their home cage after data acquisition to recover from anesthesia. The recorded waveform data were processed and analyzed, as previously described.[21,35]

Uterine Artery Isolation and Myogenic Tone Assessment

Animals were euthanized by deep anesthesia with ketamine/xylazine (ketamine; 43 mg kg^{-1}, i.p., and xylazine; 6 mg kg^{-1}, i.p.) followed by cervical dislocation. As previously described,[21] the uterus was harvested, rinsed, and quickly placed in chilled Ca^{2+}-free HEPES buffer of the following composition (in mmol L^{-1}): 140 NaCl, 5 KC1, 1.2 $MgSO_4$, 10 NaAcetate, 10 HEPES, 1.2 $Na_2H_2PO_4$, 5 dextrose, with pH adjusted to 7.4 with NaOH. Segments of the main UA were dissected and cleaned of perivascular fat, excised, and transferred into a Living Systems CH-1-LIN Vessel Chamber (Catamount, Burlington, VT) containing Ca^{2+}-free HEPES buffer. Each artery segment was cannulated at both ends with glass pipettes and secured with double nylon ligature. The vessel lumen was perfused with Ca^{2+}-free HEPES buffer without or with 1 M L-NAME. The chamber containing the vessel preparation was placed on Ti Eclipse Nikon inverted microscope equipped with IonOptix vessel dimensions data acquisition system. The bath fluid was then switched to Ca^{2+}-containing HEPES buffer and warmed with a servo-controlled heating system. After the bath temperature had risen to at least 35°C, the intraluminal pressure was increased to and maintained at 60 mm Hg with a servo-controlled pump system connected to the mounted vessel preparation via an in-line pressure transducer filled with Ca^{2+}-free HEPES buffer. After 5 min of equilibration, vessel viability was tested by abluminal application of 2 concentrations (15 and 60 mM) of prewarmed potassium chloride (KCl)-HEPES buffer. Artery segments with less than 50% reduction in lumen diameter in response to 60 mM KCl were discarded. Approximately 10 min after the viability test, the artery segments were incubated with HEPES buffer containing vehicle, dopamine (DA, 10 μM), dibutyryl cyclic-AMP (Db-cAMP, 10 μM) for 20 min, or pertussis toxin (PTX, 200 ng mL^{-1}) for 2 h. To evoke myogenic constriction, intraluminal pressure was increased stepwise from 20 to 160 mm Hg (20-mm Hg increments from 20 mm Hg, 5 min each), while lumen and vessel diameters were continuously tracked with IonOptix edge detection system, as previously described.[42] After the highest-pressure step, the vessels were incubated in Ca^{2+}-free HEPES buffer containing 1 mM EGTA for 20 min at 60 mm Hg.

The pressure steps were then repeated as described above to determine passive diameter at each intraluminal pressure. Myogenic tone at each intraluminal pressure was calculated, as previously described.[21]

Measurement of Stimulated cAMP Generation in Freshly Isolated UA

Uterine arteries were freshly isolated from harvested uterine horns of nonpregnant mice, as described above, and were incubated with 3-isobutyl-1-methylxanthine (IBMX, 500 μM) in HEPES buffer at 37°C for 15 min. This was followed by a second incubation with vehicle (0.01% DMSO) control or forskolin (50 μM) in IBMX-HEPES buffer for 5 min at 37°C. Subsequently, the arteries were flash-frozen in liquid nitrogen and stored at −80°C for further processing and analysis later. Sample preparation and analysis were conducted by following the assay protocol provided by the manufacturer of the cAMP detection kit (No: ADI-900-163, Enzo Life Sciences, NY).

Measurement of PDE Activity in Freshly Isolated UA

Uterine arteries were freshly obtained from nonpregnant mice as described above. Three treatment groups were generated; specifically, untreated control, DA (10 μM, 10 min)-treated, and PTX (750 ng mL^{-1}, 2 h)-treated groups. All incubations were performed in Ca^{2+}-free HEPES buffer at 37°C. After various treatments, the arterial vessel samples were flash-frozen in liquid nitrogen and stored at −80°C for further processing and analysis later. Sample preparation and analysis were conducted in accordance with the protocol provided with the PDE Activity Assay Kit (No. ab241034, Abcam, MA).

Bulk RNA Sequencing and Transcriptomics

Uterine arteries and small branches were cleaned of all perivascular fat and excised from the uterine horns of nonpregnant WT, *Rgs2*$^{-/-}$, *Rgs5*$^{-/-}$, and *Rgs2/5* dbKO mice in chilled HEPES buffer as described above. Three samples, each comprising pooled vessels from 3 mice, of each genotype were processed for RNA isolation using the RNeasy Mini Kit (QIAGEN) by following the manufacturer's protocol, which included the sample treatment with DNase I to remove potential genomic DNA contamination. Initial RNA quality was examined using a NanoDrop 2000 Microvolume Spectrophotometer (Thermo Fisher Scientific). Ribonucleic acid quality control and library preparation were performed by the Case Western Reserve University Genomics Core facility (https://genomics.case.edu) using an Invitrogen Qubit Fluorometer RNA assay with an AATI Fragment Analyzer RNA assay to determine concentration and the integrity of RNA and an Illumina NextSeq High Output Flow Cell—1 × 75 bp run, respectively, as previously described.[43] FastQ files were transferred to the Case Western Reserve University Institute for Computational Biology for sequence alignment and transcriptional analysis using ADVAITA next-generation bioinformatics software. Signaling pathway and gene ontology (GO) analysis for the identification of enriched terms and overrepresented genes in sets of genes with measured expression were performed using *iPathwayGuide*, as previously described.[43] Genes in WT samples were used as a reference to determine differential expression (DE) in each knockout genotype. Genes considered to have DE were those with ≥0.6-fold change in measured expression (ME) relative to the expression in WT tissue. A P-value < .05 threshold for a Pathway gene was considered to be significantly altered.

Chemical Reagents

All reagents were purchased from Sigma-Aldrich, unless indicated otherwise. Pertussis toxin (200 or 750 ng mL^{-1}), an adenosine diphosphate (ADP)-ribosylating agent, was used to specifically inactivate $G_{i/o}$ class G proteins. Dibutyryl cyclic-AMP, sodium salt (10 μM; Tocris Bioscience, MN, USA) was applied as exogenous cAMP. Dopamine (10 μM; Tocris Bioscience, MN, USA) was used to stimulate D_2-like DA receptors for the activation of $G_{i/o}$ class G proteins. IBMX was used as a pan-PDE inhibitor.

Data and Statistical Analysis

All data are mean ± SE. All statistical analyses were performed using GraphPad Prism software version 10.1.1. Normality of data distribution was tested using the Shapiro-Wilk test, while the ROUT method (Q = 5%) was used for outlier tests. Unpaired Student's t-test was used for the comparison of baseline parameters. For the assessment of within-group effects of various drug treatments on myogenic tone, one-way analysis of variance (ANOVA) mixed effect model was used, and two-way ANOVA mixed effect model was used for between-group comparisons, each followed by Sidâk post hoc tests. The calculation of the effective intraluminal pressure eliciting a half-maximal myogenic constriction (EiP_{50}) and maximal myogenic constriction (E_{max}) was performed using sigmoidal, 4PL nonlinear curve fitting, where X and Y values were the applied pressure steps and the corresponding myogenic constriction, respectively, in GraphPad Prism software. The level of significance was set at $P < .05$.

Results

Deletion of RGS2 and RGS5 Leads to Differential Uterine Hemodynamic Response to Nitric Oxide Synthase Inhibition

Previously, we showed that signaling via the inhibitory G protein, $G_{i/o}$ class G proteins, promotes myogenic constriction, and that increased $G_{i/o}$ activity in nonpregnant *Rgs2*$^{-/-}$ mice contributes to augmented myogenic tone, increased impedance, and decreased UBF velocity.[21] However, to the extent that diminished vasodilation and/or impaired $G_{i/o}$ regulation by other RGS proteins contributes to decreased uterine perfusion in *Rgs2*$^{-/-}$ mice is not clear. To address these questions, we assessed UBF by Doppler US in mice lacking *Rgs5*, which belongs to the same RGS family as *Rgs2*, and mice dually lacking *Rgs2* and 5, and treated with or without acute systemic blockade of nitric oxide synthase (NOS) with L-NAME. At baseline, and prior to L-NAME administration, peak systolic velocity (PSV) was reduced in *Rgs2/5* dbKO mice and trended lower in *Rgs2*$^{-/-}$and *Rgs5*$^{-/-}$ relative to WT mice. In contrast, end diastolic velocity (EDV) was similar in all genotypes (Figure 1). Baseline mean pressure gradient of flow trended lower in *Rgs2*$^{-/-}$ and *Rgs5*$^{-/-}$ mice and was markedly decreased in *Rgs2/5* dbKO relative to WT mice. Baseline indices of impedance, including resistivity index (RI), pulsatility index (PI), and PSV/EDV ratio, were more variable among the genotypes. At baseline, RI, PI, and PSV/EDV ratio were similar among WT, *Rgs2*$^{-/-}$, and *Rgs5*$^{-/-}$ mice but trended lower in *Rgs2/5* dbKO mice. A bolus administration of L-NAME decreased PSV in all genotypes, though the effect appeared to be less pronounced in *Rgs5*$^{-/-}$ and *Rgs2/5*

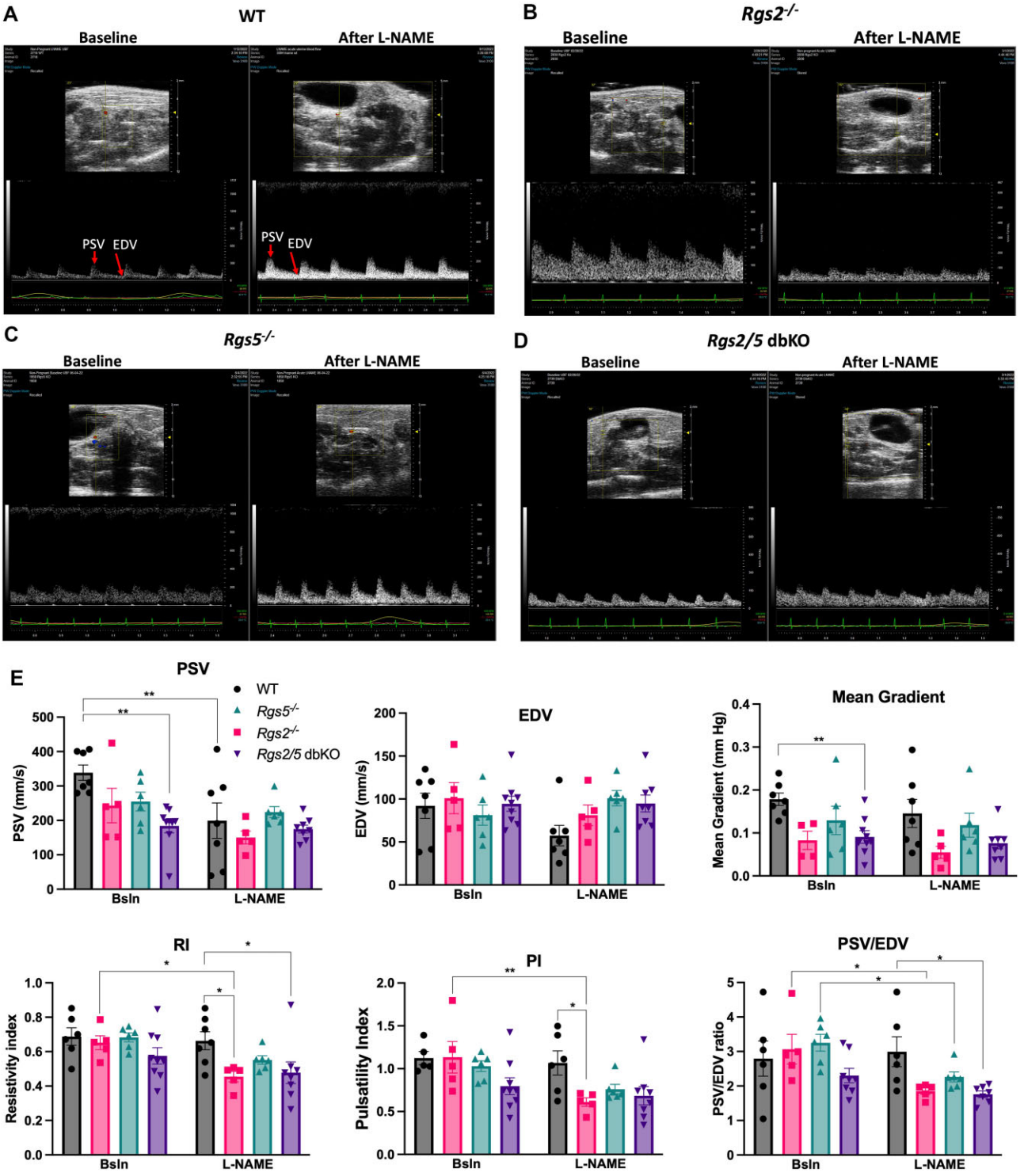

Figure 1. The effects of nitric oxide synthase blockade on uterine blood flow in mice null for *Rgs2* (*Rgs2*$^{-/-}$) or *Rgs5* (*Rgs5*$^{-/-}$), or dually lacking *Rgs2* and 5 (*Rgs2/5* dbKO) as assessed by transabdominal Doppler ultrasound. (**A**-**D**) Representative uterine blood flow sonograms of pulsed Doppler and flow waveforms of uterine artery Doppler ultrasonography at baseline (Bsln) and ~10 min after intraperitoneal injection of L-N^{G}-Nitroarginine methyl ester (L-NAME, 60 mg kg^{-1}, i.p.). Uterine arteries were located behind the bladder, guided by pulsed Doppler and the shape of the waveforms. Cines of the pulsed waveforms were acquired at an angle of ~30° and frequency of 24 Hz. (**E**) Summary bar graphs of peak systolic velocity (PSV), end diastolic velocity (EDV), and mean pressure gradient, and the accompanying resistivity index (RI), pulsatility index (PI), and PSV/EDV ratio all derived from an average of at least 3 waveforms per animal per treatment condition. Values are mean ± SEM. Each data point represents 1 animal per genotype per group. *, **$P < .05, .01$.

dbKO mice. In contrast, only in WT mice showed a decreasing trend in EDV following L-NAME administration. Interestingly, whereas L-NAME modestly lowered mean gradient only in *Rgs2*$^{-/-}$ mice, it decreased the indices of impedance in all genotypes, except in WT mice. These data suggested that the deletion of *Rgs2*, *Rgs5*, or both *Rgs* genes had differential effects on uterine artery hemodynamics response to NOS blockade in nonpregnant mice.

The Loss of RGS5 Decreases Uterine Artery Basal Tone and Myogenic Response

Despite the evidence that RGS2, 4, and 5, all of which are members of the R4/B family, are expressed in the uterine vascular bed,[35] only RGS2 and 5 have been shown to be crucial to the regulation of G protein-dependent vasoconstriction of arteries in this vascular bed.[20,21,35] In the uterine vascular bed, the mRNA expression ratio of RGS2:RGS5 is ~1:30,[35] yet the deletion of *Rgs2* leads to increased myogenic constriction and decreased UBF,[21] while the deletion of *Rgs5* has been shown to increase vasoconstriction evoked with angiotensin II.[20] Whether RGS2 and 5 adopt similar regulatory mechanisms to finetune G protein signaling and myogenic tone in the uterine vascular bed to maintain normal uterine perfusion has not been explored. To test this hypothesis, we used ex vivo pressure myography to assess basal tone and myogenic response in UA from nonpregnant WT and *Rgs5*$^{-/-}$ mice. As shown in Table 1, basal tone was unexpectedly reduced in UA from *Rgs5*$^{-/-}$ mice relative to WT control. Similarly, myogenic constriction induced by stepwise increases in intraluminal pressure was also suppressed in *Rgs5*$^{-/-}$ UA; however, sensitivity to increases in intraluminal pressure, defined as the effective intraluminal pressure inducing half-maximal myogenic constriction (EiP_{50}), was not affected by the deletion of *Rgs5* (Figure 2A and Table 1). To determine whether increased endothelium-dependent vasodilation was involved in the reduced myogenic tone in *Rgs5*$^{-/-}$ UA, we examined myogenic response in the presence of the nonselective eNOS inhibitor, L-NAME. In WT UA, L-NAME had little effect, while it markedly increased basal tone (ie, myogenic response at 60 mm Hg, equivalent to in vivo pressure in the uterine vascular bed) in *Rgs5*$^{-/-}$ UA (Table 1). However, despite the augmented basal tone, myogenic tone in *Rgs5*$^{-/-}$ UA was lower relative WT UA in the presence of L-NAME (Figure 2B), without a significant change in the sensitivity to changes in EiP_{50} (Table 1).

The Absence of RGS5 Augments cAMP-dependent Reduction in Uterine Artery Basal Tone and Myogenic Response

Cyclic adenosine 3′,5′-monophosphate signaling is an established negative regulator of vascular tone in resistance arteries, besides endothelium-derived relaxing factors.[27,44,45] Therefore, we hypothesized that decreased myogenic response in the absence of RGS5 may be due to increased cAMP-dependent attenuation of myogenic constriction. We tested this hypothesis in 2 ways, in the presence of L-NAME: In 1 experiment, we preincubated UA with DA to stimulate $G_{i/o}$-coupled DA receptors, prior to triggering pressure-induced myogenic response. This experiment was premised on the knowledge that activation of $G_{i/o}$ directly inhibits AC, thereby decreasing cAMP generation in the vessel.[46,47] In the other experiment, UA were preincubated with exogenous cAMP to activate signaling downstream of the second messenger prior to pressure-induced myogenic response. As shown in Table 2 and compared to values in Table 1, DA elevated basal tone in both WT and *Rgs5*$^{-/-}$ UA (WT: 30 ± 9 versus 51 ± 9; *Rgs5*$^{-/-}$: 7.61 ± 4.2 versus 32 ± 12, L-NAME alone versus L-NAME + DA) such that there was no statistical difference between the 2 genotypes. Conversely, exogenous cAMP markedly decreased basal tone in WT and *Rgs5*$^{-/-}$ UA to similar levels (Table 2). Dopamine augmented the overall myogenic response but more so in *Rgs5*$^{-/-}$ UA, thereby abolishing the difference in the response between the 2 groups (Figure 3). Vessel incubation with DA also increased the sensitivity of UA to changes intraluminal pressure, which was slightly more evident in WT UA (Table 2). Conversely, exogenous cAMP decreased the overall myogenic response and abolished the difference between the 2 groups (Figure 3). Both, the sensitivity to intraluminal pressure (EiP_{50}) and maximal myogenic constriction (E_{max}) were similar between the 2 genotypes after pretreatment with Db-cAMP (Table 2).

Suppressed Myogenic Constriction in *Rgs5*$^{-/-}$ UA is Reversible By Simultaneous Deletion of *Rgs2*

The observation that $G_{i/o}$ activation with DA abolished the reduced myogenic constriction in *Rgs5*$^{-/-}$ UA suggested that the loss of RGS5, at least partly, leads to enhanced negative regulation of $G_{i/o}$ activity, thereby decreasing the activation of signaling effectors downstream of the inhibitory G protein. Previously, we showed that $G_{i/o}$-mediated facilitation of myogenic constriction is regulated by RGS2.[21] As already mentioned, RGS2 and 5 are structurally and functionally closely related,[31,34,36] and the RGS domain of both RGS proteins have been shown to directly, but independently, interact with GTP-bound $G_{i/o}$ at the same binding site in the activated Gα subunit to function as GAP.[34,48,49] Therefore, given the high RGS5:RGS2 mRNA ratio in the UA,[35] we postulated that the absence of RGS5 unmasks the tight regulation of $G_{i/o}$ by RGS2, thereby reducing the activity of downstream signaling pathways that oppose cAMP-dependent vasodilatation. To test this hypothesis, first, we determined how the absence of RGS2 affected myogenic constriction in the presence of DA activating $G_{i/o}$, or increased cAMP signaling upon the application of exogenous cAMP in UA from *Rgs2*$^{-/-}$ mice. As shown in Figure 4, myogenic response in *Rgs2*$^{-/-}$ UA was enhanced relative to WT and in contrast to the reduced response in *Rgs5*$^{-/-}$ UA, in the presence of L-NAME. And as observed in *Rgs5*$^{-/-}$ UA, the application of DA augmented myogenic constriction in *Rgs2*$^{-/-}$ UA, reaching a maximal myogenic constriction at ~80 mm Hg, while exogenous cAMP application decreased myogenic constriction (Figure 4B). We noted, however, that the application of exogenous cAMP was less robust at reducing myogenic constriction in *Rgs2*$^{-/-}$ UA relative to the effects in WT and *Rgs5*$^{-/-}$ UA, suggesting that there could be additional mechanism(s) by which RGS2 regulates myogenic response in the uterine vasculature.

Next, we reasoned that if the absence of RGS5 unmasks the GAP activity of RGS2 toward $G_{i/o}$, then the dual deletion of RGS2 and 5 should reverse the reduced myogenic response in the absence of just RGS5 as shown in Figure 2. We addressed this hypothesis by assessing myogenic response in UA from mice dually lacking RGS2 and 5 (*Rgs2/5* dbKO). Basal myogenic tone in *Rgs2/5* dbKO UA was lower compared to the level in WT but slightly higher relative to the level in *Rgs5*$^{-/-}$ UA (WT: 26 ± 8 versus *Rgs2/5* dbKO 15 ± 4 versus *Rgs5*$^{-/-}$: 7.6 ± 4). In the presence of L-NAME, basal myogenic tone almost tripled in *Rgs2/5* dbKO UA

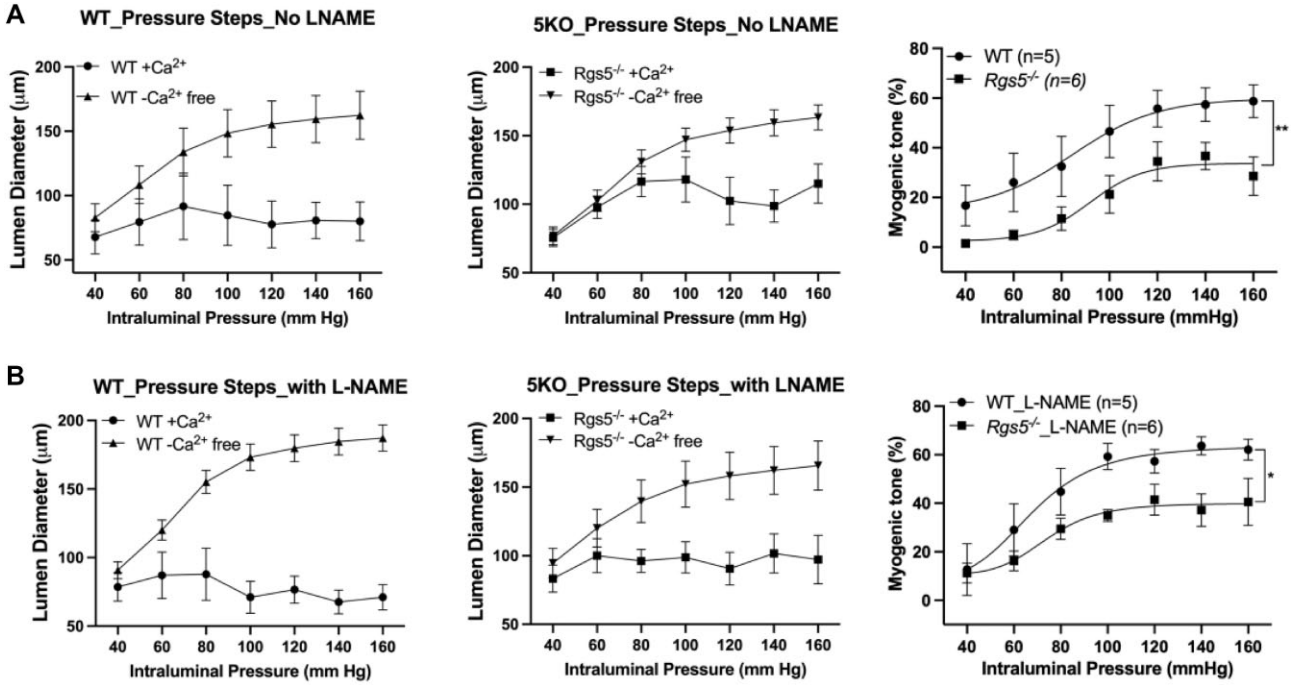

Figure 2. The absence of RGS5 decreases uterine artery myogenic response to step increases in intraluminal pressure. Lumen diameter and maximal myogenic tone of uterine arteries from wild type (WT) and *Rgs5* knockout (*Rgs5*$^{-/-}$) mice measured at increasing intraluminal pressure in the presence (**A**) and absence (**B**) of the nonselective endothelial nitric oxide synthase inhibitor, L-N^{G}-Nitroarginine methyl ester (L-NAME, 1 mM). Myogenic tone at each intraluminal pressure was calculated as a % change (%) in lumen diameter in the presence of Ca^{2+} (active diameter) relative to passive lumen diameter measured at the same intraluminal pressure in the absence of Ca^{2+} in the superfusing physiological saline solution (PSS). Values are mean ± SEM. $^{*,**}P < .05, .01$, main effect of WT versus *Rgs5*$^{-/-}$.

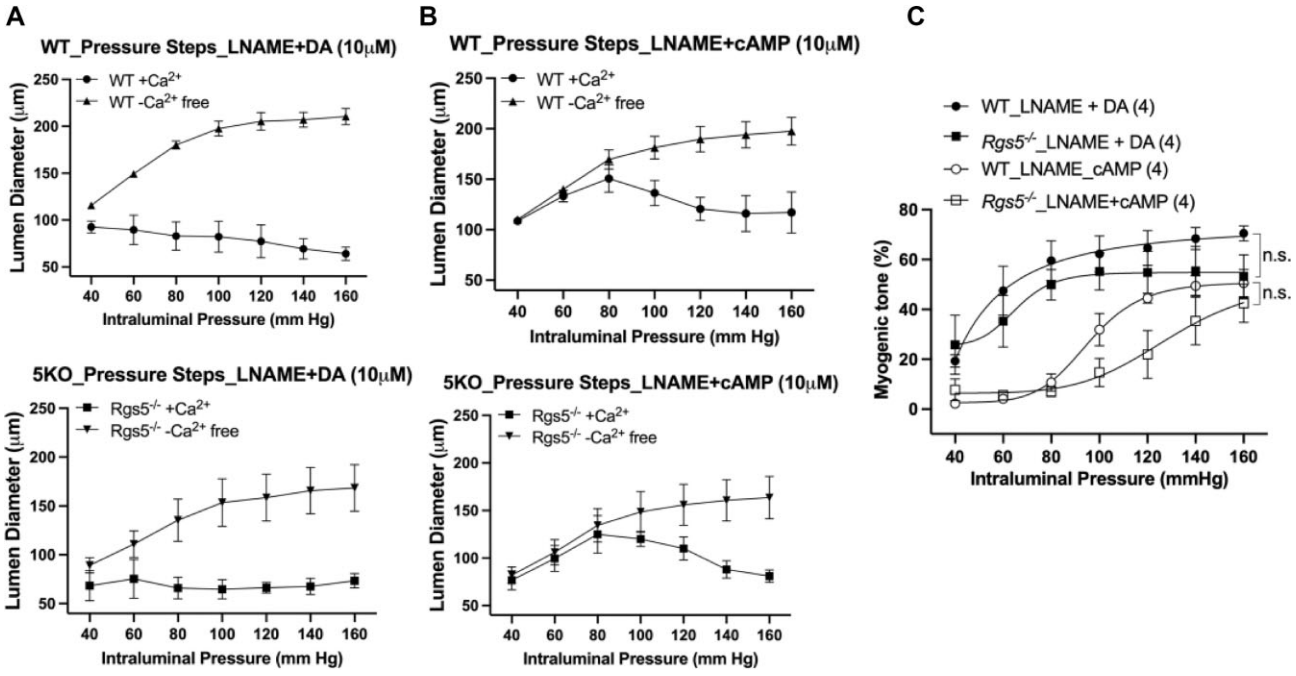

Figure 3. The absence of RGS5 facilitates modulation of myogenic response by cAMP in uterine arteries. Lumen diameter (**A** and **B**) and maximal myogenic tone (**C**) of uterine arteries from wild type (WT) and *Rgs5* knockout (*Rgs5*$^{-/-}$) mice measured at increasing intraluminal pressure in the presence of L-NAME (1 mM) with dopamine (DA, 10 μM) or exogenous cAMP (Db-cAMP, 10 μM). Myogenic tone at each intraluminal pressure was calculated as a % change (%) in lumen diameter in the presence of Ca^{2+} (active diameter) relative to passive lumen diameter measured at the same intraluminal pressure in the absence of Ca^{2+} in the superfusing physiological saline solution (PSS). Values are mean ± SEM. n.s.—not significant.

Table 1. Baseline myogenic tone, EiP_{50}, and maximal myogenic constriction of uterine arteries from nonpregnant WT and *Rgs5*$^{-/-}$ mice in the absence and presence of L-NAME

	Intraluminal Ca^{2+}-free HEPES			Intraluminal Ca^{2+}-free HEPES + L-NAME (1 mM)		
	WT ($n = 5$)	*Rgs5*$^{-/-}$ ($n = 6$)	*P*-value	WT ($n = 5$)	*Rgs5*$^{-/-}$ ($n = 6$)	*P*-value
Basal myogenic tone @ 60 mm Hg (%)	30 ± 9	7.61 ± 4.2	0.0324	24 ± 13	34 ± 8	0.2498
Half-maximal effective intraluminal pressure (EiP_{50}) (mm Hg)	84 ± 14	87 ± 5	0.4079	71 ± 7	87 ± 11	0.1198
Maximal myogenic constriction, E_{max} (%)	60 ± 7	38 ± 5	0.0188	61 ± 3	40 ± 5	0.0026

Values are mean ± SEM.

Table 2. Baseline myogenic tone, EiP_{50}, and maximal myogenic constriction of uterine arteries from nonpregnant WT and *Rgs5*$^{-/-}$ mice in the presence of L-NAME + dopamine (10 μM) or L-NAME + Db-cAMP (10 μM).

	Intraluminal Ca^{2+}-free HEPES + L-NAME + dopamine (10 μM)			Intraluminal Ca^{2+}-free HEPES + L-NAME + Db-cAMP (10 μM)		
	WT ($n = 4$)	*Rgs5*$^{-/-}$ ($n = 4$)	*P*-value	WT ($n = 5$)	*Rgs5*$^{-/-}$ ($n = 3$)	*P*-value
Basal myogenic tone @ 60 mm Hg (%)	51 ± 9	32 ± 12	0.1238	7 ± 3	4 ± 3	0.2341
Half-maximal effective intraluminal pressure (EiP_{50}) (mm Hg)	46 ± 17	71 ± 2	0.1810	100 ± 8	115 ± 12	0.2107
Maximal myogenic constriction, E_{max} (%)	69 ± 6	60 ± 4	0.1567	52 ± 5	48 ± 2	0.2280

Values are mean ± SEM.

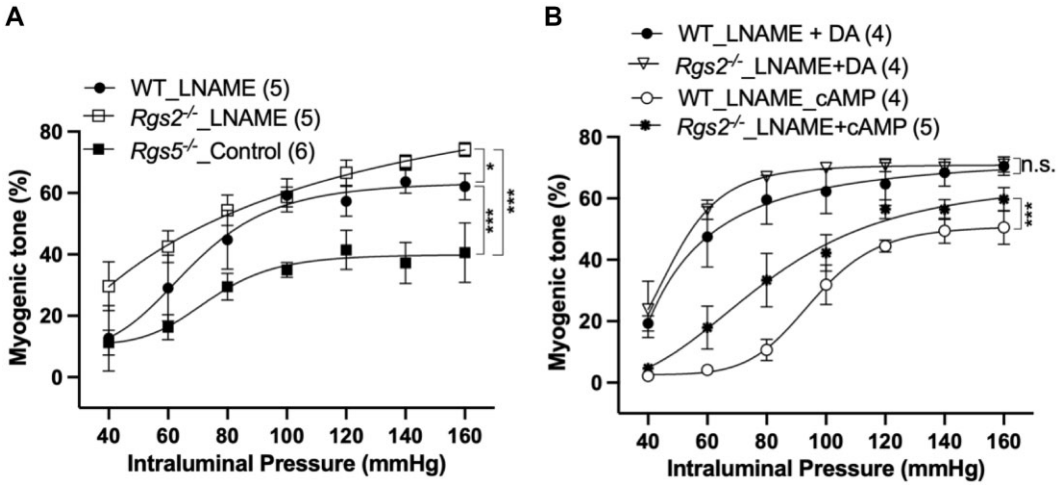

Figure 4. The absence of RGS2 augments myogenic response partly due to reduced cAMP-dependent vasodilation in uterine arteries. (**A**) Maximal myogenic tone of uterine arteries from *Rgs2* knockout (*Rgs2*$^{-/-}$) mice compared to those of wild type (WT) and *Rgs5* knockout (*Rgs5*$^{-/-}$) mice determined at increasing intraluminal pressure in the presence of 1 mM L-NAME. (**B**) Maximal myogenic tone of uterine arteries from WT and *Rgs2*$^{-/-}$ mice determined at increasing intraluminal pressure in the presence of 1 mM L-NAME, with or without preincubation with exogenous cAMP (Db-cAMP, 10 μM). Myogenic tone at each intraluminal pressure was calculated as a % change (%) in lumen diameter in the presence of Ca^{2+} (active diameter) relative to passive lumen diameter measured at the same intraluminal pressure in the absence of Ca^{2+} in the superfusing physiological saline solution (PSS). Values are mean ± SEM. n.s.—not significant; *, ***$P < .05, .001$.

(WT: 24 ± 13 versus *Rgs2/5* dbKO 47 ± 14 versus *Rgs5*$^{-/-}$: 34 ± 8). Step increases in intraluminal pressure elicited a greater myogenic response in *Rgs2/5* dbKO UA relative to the response in *Rgs5*$^{-/-}$ UA but similar to the response in WT UA in the absence or presence of L-NAME (Figure 5A and B). The application of DA or exogenous cAMP, respectively, augmented or decreased myogenic response in *Rgs2/5* dbKO UA as observed in WT and *Rgs2*$^{-/-}$ UA (Figure 5C). Interestingly, the decline in the maximal myogenic response in the presence of exogenous cAMP appeared more pronounced in *Rgs2/5* dbKO relative to WT UA. Together, these results indicated that the absence of RGS5 disinhibits the modulation of UA myogenic tone by RGS2 by facilitating cAMP-dependent vasodilatation.

Deletion of *Rgs2* and 5 Alters the Expression of Genes Involved in cAMP, Calcium, and Contractile Signaling in the Uterine Vascular Bed

To identify the signaling pathway(s) potentially involved in the differential effects of the absence of RGS2 and 5 on uterine artery myogenic tone, we performed bulk RNA sequencing (RNA-seq) to determine how the deletion of *Rgs2*, *Rgs5*, or both *Rgs2* and *Rgs5* simultaneously altered the UA transcriptome in nonpregnant mice. The number of differentially expressed (DE) genes with ≥0.6-fold change in ME relative to the expression in WT tissue, as detected by bulk RNA-seq, was similar between UA from *Rgs2*$^{-/-}$ (DE/ME: 3076/15 985, $P < .05$), *Rgs5*$^{-/-}$ (DE/ME:

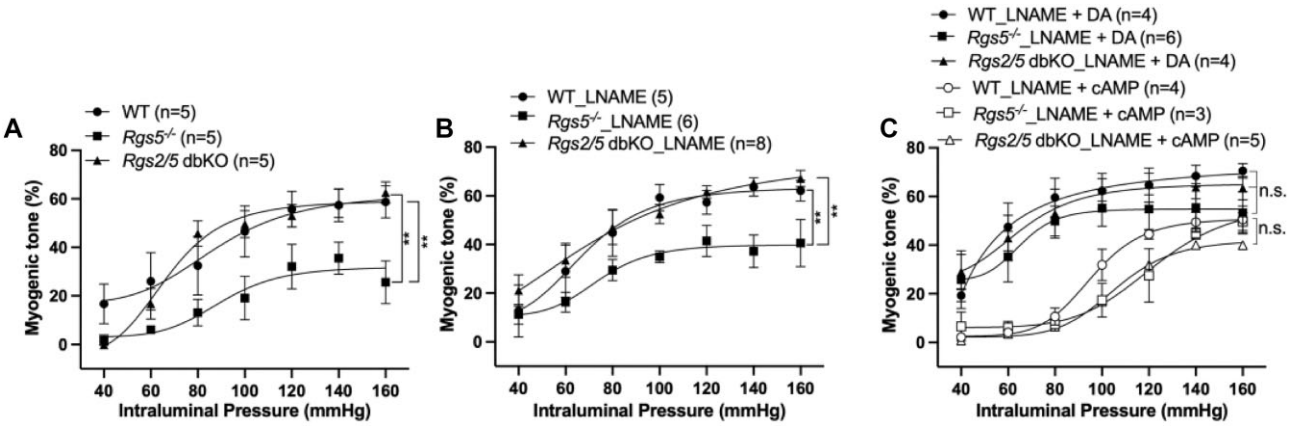

Figure 5. The dual absence of RGS2 and RGS5 abolishes the suppressed myogenic response in *Rgs5*$^{-/-}$ uterine arteries partly via the attenuation of cAMP-dependent vasodilation. (**A** and **B**) Maximal myogenic tone of uterine arteries from *Rgs2*/5 double knockout (*Rgs2*/5 dbKO) mice compared to those of wild type (WT) and *Rgs5* knockout (*Rgs5*$^{-/-}$) mice determined at increasing intraluminal pressure in the presence and absence of 1 mM L-NAME. (**C**) Maximal myogenic tone of uterine arteries from WT and *Rgs5*$^{-/-}$, and *Rgs2*/5 dbKO mice determined at increasing intraluminal pressure in the presence of 1 mM L-NAME, with or without preincubation with dopamine (DA, 10 μM) or exogenous cAMP (Db-cAMP, 10 μM). Myogenic tone at each intraluminal pressure was calculated as a % change (%) in lumen diameter in the presence of Ca^{2+} (active diameter) relative to passive lumen diameter measured at the same intraluminal pressure in the absence of Ca^{2+} in the superfusing physiological saline solution (PSS). Values are mean ± SEM. n.s.—not significant; $^{**}P < .01$.

3095/15 962, $P < .05$), and *Rgs2*/5 dbKO (DE/ME: 3754/16 099, $P < .05$) mice. Among the 3 knockout groups, *Rgs2*/5 dbKO had the most DE genes exclusive to that genotype, while *Rgs5*$^{-/-}$ had the least (Figure 6A). From pathway analysis, we found the following signaling pathways with DE genes: cAMP, calcium, vascular smooth muscle contraction, and extracellular matrix (ECM)-receptor interaction, to be among the top 6 pathways differentially altered by single or dual deletion of *Rgs2* and 5, with calcium and cAMP signaling pathways being common among all 3 knockout genotypes (Figure 6B-D). Given the observed effect of exogenous cAMP in normalizing myogenic tone in UA from *Rgs2*$^{-/-}$ and *Rgs2*/5 dbKO mice, we focused on further examining DE genes in the cAMP pathway to determine how the deletion of *Rgs2*, *Rgs5*, or both *Rgs* genes altered the expression of genes in this pathway. In *Rgs2*$^{-/-}$ UA, 6 genes were upregulated, while 10 genes were downregulated; in *Rgs5*$^{-/-}$ UA, 11 genes were upregulated, while 9 genes were downregulated; and in *Rgs2*/5 dbKO UA, 10 genes were upregulated, while 6 genes were downregulated (Figure 6E-G). The DE genes in the cAMP signaling pathway included those for G_s- and $G_{i/o}$-coupled GPCRs, AC, protein kinase A, calmodulin kinases, and PDEs. Of note, *Rgs5*$^{-/-}$ UA showed increased expression of *Adcy*5 and 6, which encode the 2 most abundant AC isoforms in the mouse uterine vascular bed (Figure S1). Interestingly, all the DE cAMP signaling pathway genes in *Rgs2*/5 dbKO UA were altered in similar directions in either *Rgs2*$^{-/-}$ or *Rgs5*$^{-/-}$ UA, except the adenosine receptor 2a gene, *Adora2a*, which was exclusively upregulated in *Rgs2*/5 dbKO UA (Figure 6G).

Phosphodiesterase Activity Mediates $G_{i/o}$-dependent Downregulation of cAMP Signaling and Augmented Basal Tone and Myogenic Response in UA From *Rgs2*$^{-/-}$ and *Rgs2*/5 dbKO Mice

The results from the UA transcriptome and pathway analysis showing upregulation of *Adcy*5 and 6, coupled with the downregulation of genes encoding various PDE isoforms suggested signaling imbalance in favor of upregulated cAMP level and/or signaling in *Rgs5*$^{-/-}$ UA. In addition, the observation that exogenous cAMP decreased myogenic constriction in WT UA to similar levels in *Rgs5*$^{-/-}$ UA also suggested that reduced UA myogenic tone in the absence of RGS5 was due at least partly to increased cAMP-dependent smooth muscle relaxation. Moreover, Db-cAMP, the cAMP analogue utilized in this study, elicits its effect partly by inhibiting PDE activity.[50,51] Together, these observations led to the postulation that the absence of RGS5 dampens the enhancement of PDE activity by $G_{i/o}$ signaling, thus decreasing cAMP degradation to promote cAMP-mediated vasodilatation and reduce myogenic tone. To test this hypothesis, first, we examined the effects of the pan-PDE inhibitor, IBMX, and $G_{i/o}$ inhibition with PTX (750 ng mL^{-1}) on basal tone and myogenic response in UA from WT, *Rgs2*$^{-/-}$, and *Rgs5*$^{-/-}$ mice. IBMX concentration-dependently reduced the maximal myogenic constriction and caused a rightward shift of the pressure-myogenic response curve in all genotypes (Figure 7). Interestingly, myogenic response in UA from *Rgs2*$^{-/-}$ mice was more sensitive to the lowest concentration of IBMX, while incubation with 10 μM of the PDE inhibitor almost completely abolished myogenic constriction in all genotypes (Figure 7A-C). Moreover, PTX-mediated inactivation of $G_{i/o}$ decreased basal tone and myogenic response in all genotypes but more substantially in UA from WT, *Rgs2*$^{-/-}$, and *Rgs2*/5 dbKO mice (Figure 7D). Next, we determined whether increased sensitivity of UA myogenic tone in the absence of RGS2 was due to enhanced inhibition of cAMP generation and/or the upregulation of PDE activity due to increased $G_{i/o}$ activity. As shown in Figure 8A, forskolin-induced cAMP generation trended downward in UA from *Rgs2*$^{-/-}$, and *Rgs2*/5 dbKO mice, relative to levels in WT UA. In contrast, UA lacking *Rgs5* showed a trend toward enhanced forskolin-induced cAMP generation. Conversely, basal PDE activity in *Rgs2*$^{-/-}$ or *Rgs2*/5 dbKO UA was augmented relative to the activity in WT UA (Figure 8B). In *Rgs5*$^{-/-}$ UA, basal PDE activity trended higher relative to WT level; however, the difference did not reach statistical significance (Figure 8B). To test whether the augmented PDE activity was a consequence of enhanced $G_{i/o}$ signaling, PDE activity in the UA was examined in vessels preincubated with PTX (750 ng m−1, 2 h). $G_{i/o}$ inactivation had no effect on PDE activity in UA from WT or *Rgs5*$^{-/-}$ UA but markedly reduced the

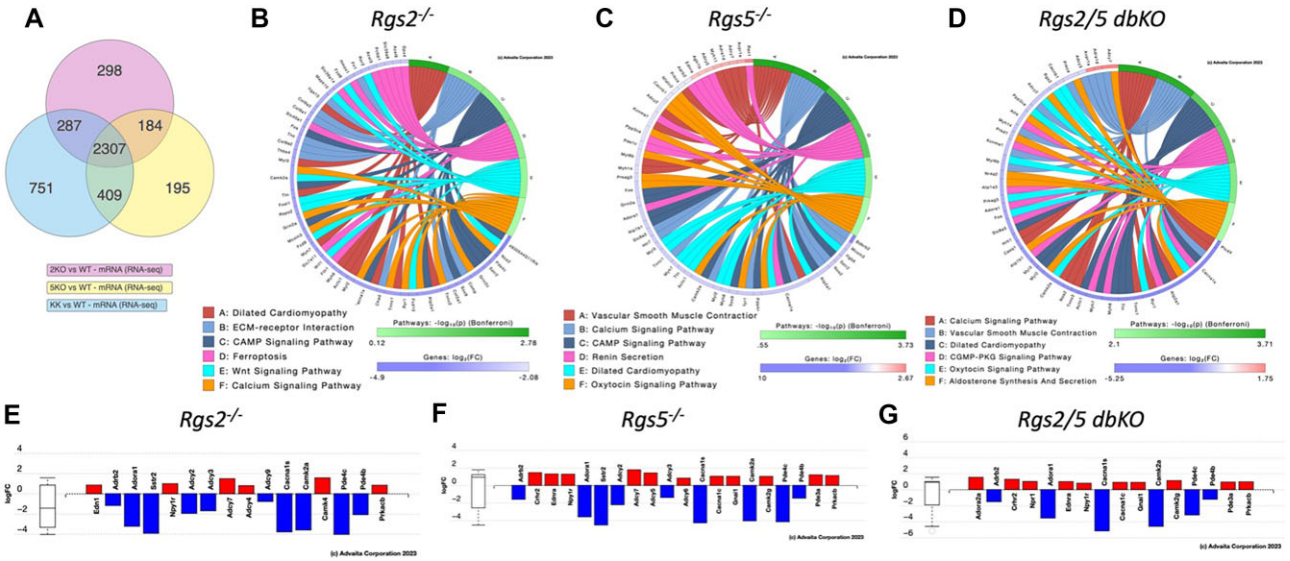

Figure 6. Effects of single or dual deletion of *Rgs2* and *Rgs5* on the transcriptional profiles of genes in signaling pathways involved in the regulation of smooth muscle contractility in the uterine vascular bed. (**A**) Venn diagram showing the number of genes, as detected by bulk RNA sequencing, with differential expression (DE) in uterine arteries from *Rgs2* knockout (2KO or *Rgs2*$^{-/-}$), *Rgs5* knockout (5KO or *Rgs5*$^{-/-}$), and *Rgs2/5* double knockout (KK or *Rgs2/5* dbKO) mice relative to the expression in arteries from wild type (WT) mice. The numbers in the nonoverlapping areas of the circles indicate the number of genes with altered expression specific to the single or dual silencing of *Rgs2* and/or *Rgs5*. (**B-D**) Signaling network analysis showing the top 6 pathways and the most prominent genes with differentially altered expression. The color scheme depicts the signaling pathways and the range of fold change in gene expression. (**E-G**) Differentially expressed pathway genes in the cAMP signaling pathway. The selected genes are those with ≥0.6-fold change in DE and $P < .05$ and encoding proteins reported to be involved in the regulation of cAMP levels including generation and degradation. Red and blue bars indicate upregulation and downregulation, respectively.

activity in *Rgs2*$^{-/-}$ UA close to the level in WT UA (Figure 8C). In *Rgs2/5* dbKO UA, PTX treatment reduced PDE activity slightly but remained markedly elevated relative to the level in WT UA. Together, these results demonstrated that RGS2 and 5 modulate myogenic tone in UA, at least partly, by controlling $G_{i/o}$-dependent regulation of cAMP levels.

Discussion

The findings in the current study provide new lines of evidence that finetuning of G protein signaling in the uterine vascular bed by RGS proteins is key to the regulation of uterine artery hemodynamics and blood flow. The novel signaling pathway identified herein is that $G_{i/o}$ upregulates PDE activity that, in turn, decreases the attenuation of myogenic tone by cAMP signaling in UA. To our knowledge, this is the first evidence that RGS proteins regulate myogenic tone through mechanisms that involve (1) the canonical negative regulation of $G_{i/o}$-mediated inhibition of cAMP generation and (2) the newly discovered pathway, whereby RGS2 and 5 promote cAMP signaling by dampening $G_{i/o}$-mediated augmentation of PDE activity. We further show that the effects of RGS2 and 5 on myogenic tone and uterine artery hemodynamics are reflected by changes in flow velocities and pressure gradient, as evaluated by Doppler ultrasonography, in response to changes in perfusion pressure driving flow in that vascular bed.

In the nonpregnant state, UBF serves the crucial role of facilitating endometrial growth and vascularity, as well as contributing to the readying of the endometrium for the implantation of fertilized ova.[52–54] Given that the uterine vasculature is a high resistivity vascular bed in the nonpregnant state, impedance to blood flow to the uterus is determined mostly by vascular resistance, which, in turn, is determined mainly by myogenic tone and the modulatory effects of vasodilatory factors.[9,55,56] The UA senses and responds to the cyclical stretch from systemic pressure that drives UBF, and this leads to the generation of a 2-component flow velocity Doppler waveform comprising peak systolic and end diastolic velocities, mimicking the cardiac cycle.[7,12] During early systole of the cardiac cycle in the nonpregnant state, the level of resistance to systolic blood flow is reflected by the formation of a notch following a sudden fall in flow velocity from PSV, which precedes the initiation of EDV in the UBF Doppler waveform.[12] Thus, the level of PSV and/or the prominence of the systolic notch in the UBF Doppler waveform are a reflection of the level of myogenic tone and resistance in the uterine vascular bed.[7,12] The current study shows that in WT mice, both components of UBF velocity (PSV and EDV) are responsive to increased systemic pressure elicited by systemic blockade of NOS with L-NAME. Interestingly, the loss of RGS2 tended to accentuate the decreased UBF flow velocity response, with a more robust decline in PSV. The change in flow velocity response was paralleled by changes in the mean pressure gradient across the uterine vascular bed that appeared relatively robust in *Rgs2*$^{-/-}$ mice after L-NAME administration relative to WT baseline. These data suggest that the vasodilatory effect of endothelium derived nitric oxide modulates the unmasking of high resistance to UBF in the absence of RGS2. Surprisingly, however, the commonly used indices of impedance, including PI and RI, tended to decrease in all knockout animals following the elevation of perfusion pressure with L-NAME. This could be clarified by 2 observations in the study. First, all 3 indices of impedance are derived from some combination of PSV and EDV and are therefore subject to the extent to which the loss of RGS2 and/or 5 affects either or both velocity components. In the knockout animals, L-NAME had relatively little effect on EDV compared to WT mice, which might have decreased the PSV-EDV gap more so in the knockout than in WT mice. Second, the loss of RGS2 and 5 may have altered basal tone and

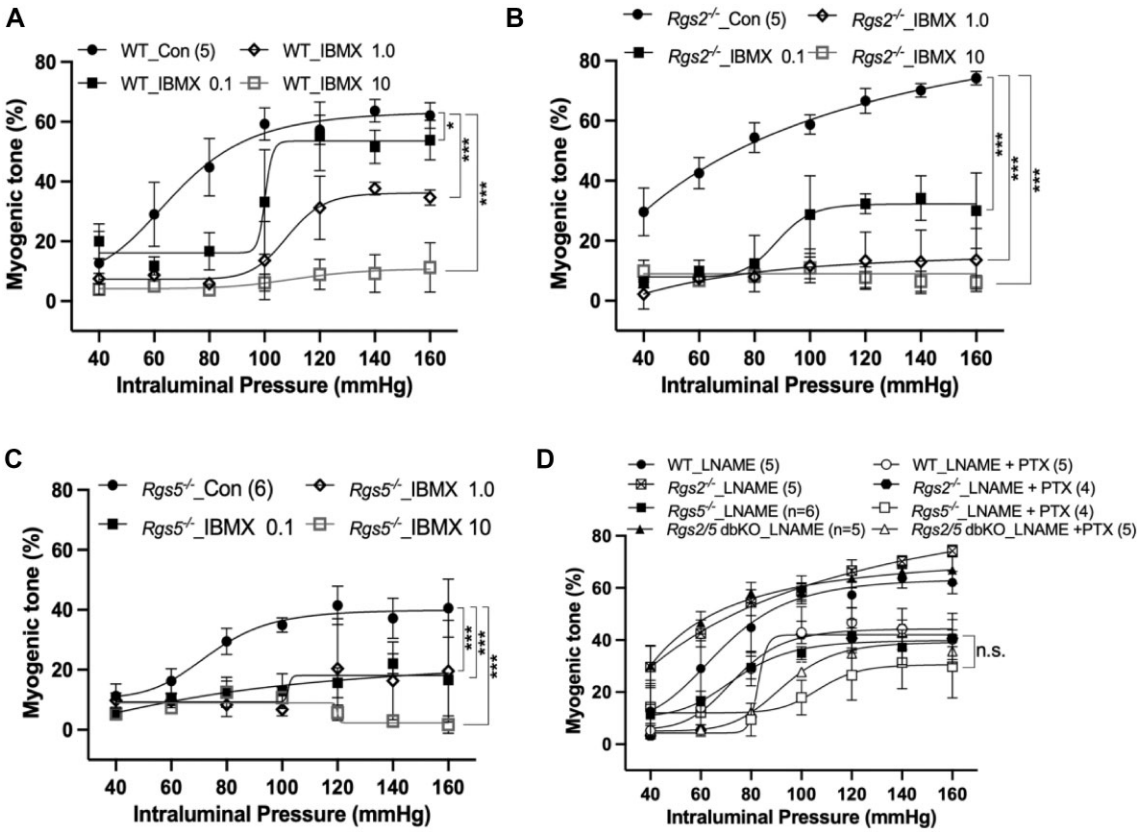

Figure 7. *Rgs2* deletion increases the sensitivity of uterine artery myogenic tone to phosphodiesterase and $G_{i/o}$ inhibition. Maximal myogenic tone of uterine arteries from wild type (WT), *Rgs2* knockout (*Rgs2*$^{-/-}$), *Rgs5* knockout (*Rgs5*$^{-/-}$), and *Rgs2/5* double knockout (*Rgs2/5* dbKO) mice determined at increasing intraluminal pressure in the presence or absence of 0.1, 1.0, or 10 μM IBMX (**A-C**) or pertussis toxin (**D**; PTX, 750 ng m−1, 2-h incubation). Myogenic tone at each intraluminal pressure was calculated as a % change in lumen diameter in the presence of Ca^{2+} (active diameter) relative to passive lumen diameter measured at the same intraluminal pressure in the absence of Ca^{2+} in the superfusing physiological saline solution (PSS). Values are mean ± SEM. n.s—not significant; $^{*,***}P < .05, .0001$.

primed the resistance vasculature to be more responsive to systolic pressure, resulting in lower PSV at baseline and in response to increased systemic pressure following NOS blockade with L-NAME. As previously reported, the loss of either RGS2 or 5 leads to endothelial dysfunction and augmented vascular reactivity to vasoactive GPCR agonists.[35,57,58] Thus, independently of changes in systemic pressure, the loss of RGS2 or 5 could lead to the attenuation of endothelium-dependent vasodilation to oppose the intrinsic myogenic constriction of the smooth muscle layer elicited by the perfusion pressure driving UBF. These effects of the absence of RGS2 and 5 may be unnoticed if impedance to flow is assessed just by quantifying the commonly used parameters of PI, RI, and PSV/EDV. As shown in this study, the results from a direct assessment of uterine artery myogenic tone using an ex vivo pressure myography further supports the hypothesis that the loss of RGS2 and 5 alters impedance to UBF by affecting the mechanisms that mediate uterine artery myogenic tone regulation, and thus vascular resistance.

In the resistance vasculature, the loss of RGS2 and 5 has been shown to enhance contractile signaling via stimulation of procontractile GPCRs such as the angiotensin type 1, α1-adrenergic, and muscarinic receptors, and impairment of the vasodilatory NO-cGMP-PKG signaling inhibiting myogenic constriction.[32,58–60] As already mentioned, we showed previously that increased myogenic constriction of UA is due partly to increased signaling via $G_{q/11}$ and $G_{i/o}$ class G proteins.[21] The findings here that the loss of RGS5 decreases uterine artery myogenic response, as opposed to the augmented response in the absence of RGS2, were counterintuitive, given the structural and functional similarities between RGS2 and 5 and that both RGS proteins act as GAP toward $G_{q/11}$ and $G_{i/o}$.[30,34,61] From a more detailed examination of $G_{i/o}$ signaling using pharmacology and transcriptomics, we find that by sheer level of expression in the uterine vasculature, RGS5 appears to act as effector antagonist, out-competing RGS2 in engaging $G_{i/o}$ but with less efficient GAP activity. This hypothesis is supported by the observation that the absence of RGS5 decreases myogenic tone and is associated with a trend toward augmented forskolin-stimulated cAMP generation, suggesting decreased competitive G protein interaction and more efficient GAP activity of RGS2 toward $G_{i/o}$. This contrasts with the enhanced myogenic tone in the absence of RGS2 that is accompanied by a decreasing trend in forskolin-stimulated cAMP production, demonstrating a less efficient regulation of $G_{i/o}$ by RGS5. Others and we have reported that this effector antagonism between multiple RGS proteins is present in ventricular myocytes and the central nervous system.[40,62] In a previous study by Garzon and colleagues, it was reported that effector antagonism by RG-R7 is involved in the delayed tolerance associated with repeated morphine administration. That is, RGS-R7 proteins were found to bind $G_{i/o/z}$ proteins and sequester them, thereby preventing the acceleration of GTP hydrolysis necessary to restrict the amplitude of opioid analgesia by the more efficient RGS-R4 and RGS-Rz.[62] In ventricular myocytes, the loss of only RGS2 or both RGS2 and 5 but

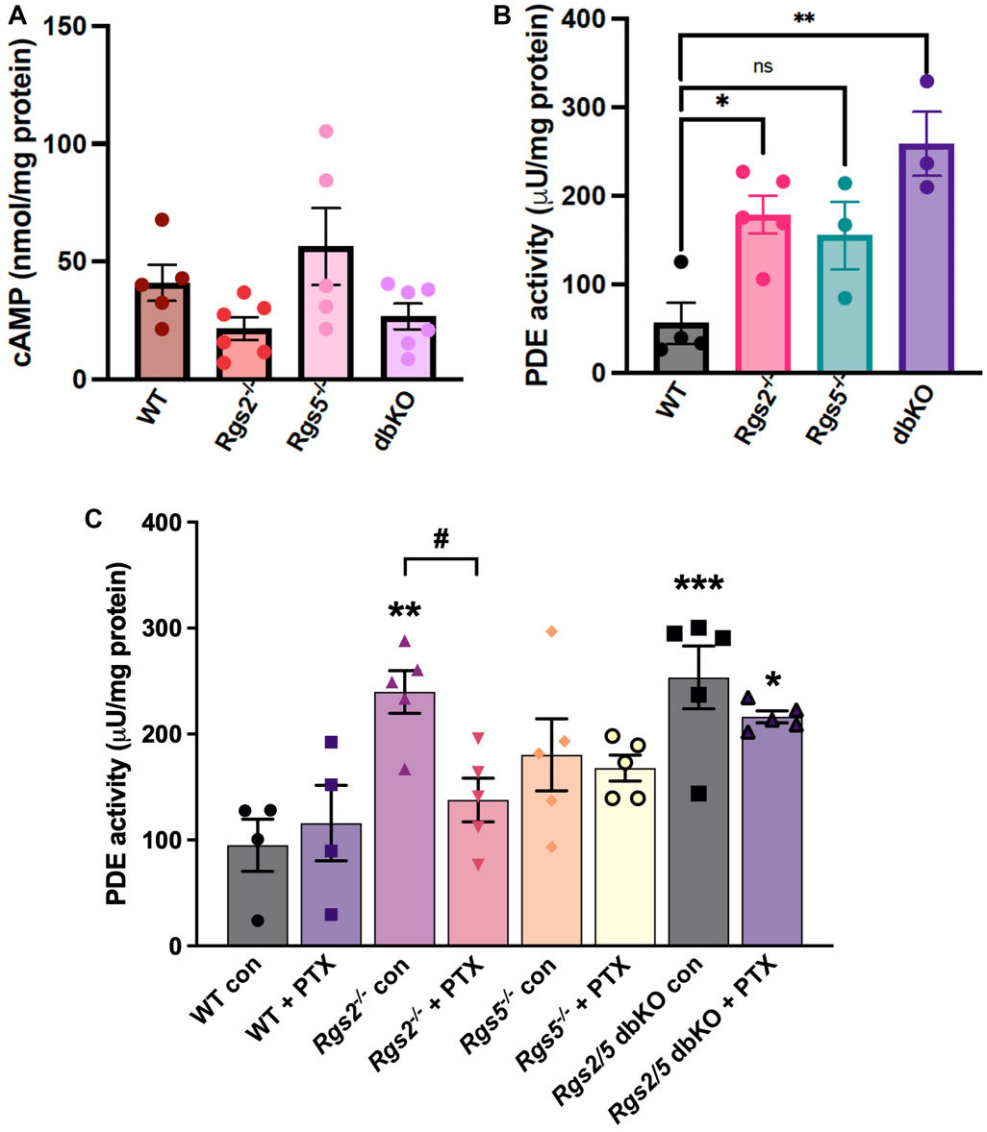

Figure 8. The loss of $G_{i/o}$ regulation by RGS2 and 5 augments uterine artery myogenic tone by downregulating cAMP generation and upregulating PDE activity. (**A**) Forskolin-stimulated cAMP generated in uterine arteries from wild type (WT), *Rgs2* knockout (*Rgs2*$^{-/-}$), *Rgs5* knockout (*Rgs5*$^{-/-}$), and *Rgs2/5* double knockout (*Rgs2/5* dbKO) mice. Freshly isolated uterine arteries were incubated with forskolin (50 μM) for 5 min in the presence of 50 μM IBMX. (**B** and **C**) Phosphodiesterase (PDE) activity in uterine arteries from WT, *Rgs2*$^{-/-}$, *Rgs5*$^{-/-}$, and *Rgs2/5* dbKO mice. Freshly isolated uterine arteries were incubated with vehicle (0.01% DMSO) or PTX (750 ng m^{-1}) for 2 h before processing for the PDE activity assay. Data points indicate assays with uterine arteries from individual mice. Values are mean ± SEM. $^{*,**}P < .05, .01$ versus WT control (con); $^{\#}P < .05$, *Rgs2*$^{-/-}$con versus *Rgs2*$^{-/-}$ + PTX; and ns—not significant.

not RGS5 alone leads to ventricular myocyte arrhythmias associated with decreased cAMP generation that is reversible by chemical inactivation of $G_{i/o}$ with PTX.[40] The results in this study also indicate that in the absence of NOS-generated nitric oxide, the modulation of $G_{i/o}$ activity by RGS2 and 5 to promote cAMP signaling is critical to preventing excessive myogenic response to changes in intraluminal pressure in the uterine vascular bed. And, besides the regulation of the canonical inhibition of cAMP generation by $G_{i/o}$, we found a novel mechanism by which RGS2 and 5 promote cAMP signaling to modulate UA myogenic tone.

Gene ontology and *iPathway* analysis of the uterine vascular bed transcriptome revealed that the absence of RGS2 or 5 leads to DE and enrichment of genes involved in the cAMP signaling pathway, consistent with the importance of the regulatory role of RGS2 and 5 of this pathway in the uterine vascular bed.[20,21] The loss of RGS5 but not RGS2 increased the enrichment of *Adcy*5 and 6, the genes encoding the most abundant AC isoforms in the uterine vascular bed, suggesting augmented cAMP generation, which is consistent with the increased trend of forskolin-stimulated cAMP generation in UA from *Rgs5*$^{-/-}$ mice. Interestingly, the absence of RGS5 also increased the enrichment of *Pde3a*, perhaps balancing the upregulated expression of AC genes to maintain balanced cAMP levels. However, chemical interrogation of cAMP signaling shows that the regulation of PDE activity is likely to be more crucial than gene expression in the modulation of uterine artery myogenic tone. The observation that UA from *Rgs2*$^{-/-}$ mice are highly sensitive to the nonselective PDE blocker, IBMX, suggests that PDE activity is elevated in the absence of RGS2. Additionally, the upregulated PDE activity in the absence of RGS2, or both RGS2 and 5 was sensitive to PTX, further indicating that $G_{i/o}$ signaling promotes PDE activity and that this signaling axis is regulatable, at least partly by

RGS2. However, whether the regulation of $G_{i/o}$-PDE signaling axis by RGS2 is strictly via its GAP activity cannot be ascertained from the results herein, since PTX barely had any effect on the augmented PDE activity in *Rgs5*$^{-/-}$ arteries. Moreover, the PDE isoform(s) activatable by $G_{i/o}$ in the uterine vascular bed remains to be identified, though PDE genes with DE in the absence of RGS2 could be candidate isoforms for future evaluation.

A few caveats limit the interpretation of our findings regarding the vascular mechanisms identified as mediators of altered uterine artery hemodynamics in the absence of RGS2 and 5. Notably, in both the in vivo and ex vivo experiments, we used mice with global deletion of *Rgs2* and 5. Both *Rgs* genes are prominently expressed in the cardiovascular system, particularly, in myocardial cells and in all compartments of the arterial wall, as well in regions of the central nervous system (CNS) involved in the regulation of sympathoexcitation and anxiety-like behaviors.[63–67] Therefore, other unknown compensatory mechanisms could blunt or contribute to the effects observed in this study. For instance, the interaction between the effects of changes in CNS activity due to the deletion of either or both *Rgs* genes and anesthetics could potentially impact uterine hemodynamics assessment under isoflurane anesthesia. In addition, the constitutive deletion of both *Rgs* genes may trigger some yet unknown developmental compensation that could account for the absence of overt developmental abnormalities or a severe hypertensive phenotype due at least partly to disinhibition of $G_{q/11}$ signaling and peripheral vascular tone, including in UA.[21,32,59,68] We also acknowledge that the relatively wide age range of the mice used in our study could potentially confound the interpretation of the uterine hemodynamics assessment results. As previously reported, aortic stiffness has been shown to decrease during the estrus phase in female mice.[69] Such variations in elastic artery stiffness with the estrous cycle, if also present in small muscular arteries such as UA, could impact vascular impedance, thereby blunting the effects of altered uterine artery myogenic tone and thus hemodynamics resulting from *Rgs2* and 5 deletions. Future experiments to further explore the novel pathways identified herein as regulators of uterine artery hemodynamics and myogenic tone should utilize animal models amenable to vascular compartment-specific deletion of *Rgs2* and 5.

In summary, perturbations in uterine artery hemodynamics due to elevated vascular tone can impair UBF and disrupt physiological myometrial remodeling for placentation in early pregnancy. Mutations that affect the expression and/or function of RGS2 and 5 are associated with abnormal vascular function and implicated in pregnancy complications hallmarked by abnormal uteroplacental perfusion.[37,70–73] Our study gives additional insights into pathways regulated by RGS2 and 5 that could be targeted as a novel therapeutic approach to enhancing uterine perfusion.

Acknowledgments

We thank all members of the Osei-Owusu laboratory for technical support.

Supplementary Material

Supplementary material is available at the *APS Function* online.

Funding

This work was supported by National Institutes of Health grants R56 DK132859-01A1 and R01 HL139754, and Craig H. Neilsen Foundation grant 382566 to P.O-O.

Conflict of Interest

None declared.

Data Availability

Data will be made available to the editors of the journal for review or query upon request. Transcriptomics data will be deposited in Figshare and made publicly available.

References

1. Anderson CM, Lopez F, Zhang HY, Pavlish K, Benoit JN. Reduced uteroplacental perfusion alters uterine arcuate artery function in the pregnant Sprague-Dawley rat. *Biol Reprod*. 2005;**72**(3):762–766.
2. Gallo DM, Poon LC, Akolekar R, Syngelaki A, Nicolaides KH. Prediction of preeclampsia by uterine artery Doppler at 20-24 weeks' gestation. *Fetal Diagn Ther*. 2013;**34**(4):241–247.
3. McClements L, Richards C, Patel N, et al. Impact of reduced uterine perfusion pressure model of preeclampsia on metabolism of placenta, maternal and fetal hearts. *Sci Rep*. 2022;**12**(1):1111.
4. Verlohren S, Niehoff M, Hering L, et al. Uterine vascular function in a transgenic preeclampsia rat model. *Hypertension*. 2008;**51**(2):547–553.
5. Abd el Aal DE, Kunzel W. Blood flow velocity in the uterine and external iliac arteries before and after termination of pregnancy. *Eur J Obstet Gynecol Reprod Biol*. 1994;**53**(1):11–16.
6. Dickey RP. Doppler ultrasound investigation of uterine and ovarian blood flow in infertility and early pregnancy. *Hum Reprod Update*. 1997;**3**(5):467–503.
7. El-Mazny A, Abou-Salem N, Elshenoufy H. Doppler study of uterine hemodynamics in women with unexplained infertility. *Eur J Obstet Gynecol Reprod Biol*. 2013;**171**(1):84–87.
8. Freeman SL, Russo M, England GC. Uterine artery blood flow characteristics assessed during oestrus and the early luteal phase of pregnant and non-pregnant bitches. *Vet J*. 2013;**197**(2):205–210.
9. Gosling RG, Lo PT, Taylor MG. Interpretation of pulsatility index in feeder arteries to low-impedance vascular beds. *Ultrasound Obstet Gynecol*. 1991;**1**(3):175–179.
10. Brands PJ, Hoeks AP, Rutten MC, Reneman RS. A noninvasive method to estimate arterial impedance by means of assessment of local diameter change and the local centerline blood flow velocity using ultrasound. *Ultrasound Med Biol*. 1996;**22**(7):895–905.
11. Jackson WF. Myogenic tone in peripheral resistance arteries and arterioles: the pressure is on! *Front Physiol*. 2021;**12**:699517.
12. Clark AR, James JL, Stevenson GN, Collins SL. Understanding abnormal uterine artery Doppler waveforms: a novel computational model to explore potential causes within the utero-placental vasculature. *Placenta*. 2018;**66**:74–81.
13. Barron C, Mandala M, Osol G. Effects of pregnancy, hypertension and nitric oxide inhibition on rat uterine artery myogenic reactivity. *J Vasc Res*. 2010;**47**(6):463–471.
14. Bird IM, Sullivan JA, Di T, et al. Pregnancy-dependent changes in cell signaling underlie changes in differential control of vasodilator production in uterine artery endothelial cells. *Endocrinology*. 2000;**141**(3):1107–1117.
15. Storment JM, Meyer M, Osol G. Estrogen augments the vasodilatory effects of vascular endothelial growth factor in the uterine circulation of the rat. *Am J Obstet Gynecol*. 2000;**183**(2):449–453.

16. Coats P, Johnston F, MacDonald J, McMurray JJ, Hillier C. Signalling mechanisms underlying the myogenic response in human subcutaneous resistance arteries. *Cardiovasc Res*. 2001;**49**(4):828–837.
17. Davis MJ, Earley S, Li YS, Chien S. Vascular mechanotransduction. *Physiol Rev*. 2023;**103**(2):1247–1421.
18. Davis MJ, Hill MA. Signaling mechanisms underlying the vascular myogenic response. *Physiol Rev*. 1999;**79**(2):387–423.
19. Edwards A, Layton AT. Calcium dynamics underlying the myogenic response of the renal afferent arteriole. *Am J Physiol Ren Physiol*. 2014;**306**(1):F34–F48.
20. Holobotovskyy V, Chong YS, Burchell J, et al. Regulator of G protein signaling 5 is a determinant of gestational hypertension and preeclampsia. *Sci Transl Med*. 2015;**7**(290):290ra88.
21. Jie L, Owens EA, Plante LA, et al. RGS2 squelches vascular $G_{i/o}$ and G_q signaling to modulate myogenic tone and promote uterine blood flow. *Physiol Rep* 2016;**4**(2):e12692–e12704.
22. Mederos y Schnitzler M, Storch U, Meibers S, et al. G_q-coupled receptors as mechanosensors mediating myogenic vasoconstriction. *EMBO J*. 2008;**27**(23):3092–3103.
23. Mederos YSM, Storch U, Gudermann T. Mechanosensitive $G_{q/11}$ protein-coupled receptors mediate myogenic vasoconstriction. *Microcirculation*. 2016;**23**(8):621–625.
24. Owens EA, Jie L, Reyes BAS, Van Bockstaele EJ, Osei-Owusu P. Elastin insufficiency causes hypertension, structural defects and abnormal remodeling of renal vascular signaling. *Kidney Int*. 2017;**92**(5):1100–1118.
25. Scholz N, Monk KR, Kittel RJ, Langenhan T. Adhesion GPCRs as a putative class of metabotropic mechanosensors. *Handb Exp Pharmacol*. 2016;**234**:221–247.
26. Mladenov MI, Hristov KL, Dimitrova DZ, et al. Ghrelin signalling in guinea-pig femoral artery smooth muscle cells. *Acta Physiol (Oxf)*. 2008;**194**(3):195–206.
27. Morgado M, Cairrao E, Santos-Silva AJ, Verde I. Cyclic nucleotide-dependent relaxation pathways in vascular smooth muscle. *Cell Mol Life Sci*. 2012;**69**(2):247–266.
28. Petitcolin MA, Spitzbarth-Regrigny E, Bueb JL, Capdeville-Atkinson C, Tschirhart E. Role of G(i)-proteins in norepinephrine-mediated vasoconstriction in rat tail artery smooth muscle. *Biochem Pharmacol*. 2001;**61**(9):1169–1175.
29. Chidiac P, Roy AA. Activity, regulation, and intracellular localization of RGS proteins. *Recept Channels*. 2003;**9**(3): 135–147.
30. Anger T, Klintworth N, Stumpf C, Daniel WG, Mende U, Garlichs CD. RGS protein specificity towards G_q- and $G_{i/o}$-mediated ERK 1/2 and Akt activation, in vitro. *J Biochem Mol Biol* 2007;**40**(6):899–910.
31. Bansal G, Druey KM, Xie Z. R4 RGS proteins: regulation of G-protein signaling and beyond. *Pharmacol Ther*. 2007;**116**(3):473–495.
32. Heximer SP, Knutsen RH, Sun X, et al. Hypertension and prolonged vasoconstrictor signaling in RGS2-deficient mice. *J Clin Invest*. 2003;**111**(4):445–452.
33. Hollinger S, Hepler JR. Cellular regulation of RGS proteins: modulators and integrators of G protein signaling. *Pharmacol Rev*. 2002;**54**(3):527–559.
34. Kimple AJ, Soundararajan M, Hutsell SQ, et al. Structural determinants of G-protein alpha subunit selectivity by regulator of G-protein signaling 2 (RGS2). *J Biol Chem*. 2009;**284**(29):19402–19411.
35. Koch JN, Dahlen SA, Owens EA, Osei-Owusu P. Regulator of G protein signaling 2 facilitates uterine artery adaptation during pregnancy in mice. *J Am Heart Assoc*. 2019;**8**(9): e010917.
36. Osei-Owusu P, Blumer KJ. Regulator of G protein signaling 2: a versatile regulator of vascular function. *Prog Mol Biol Transl Sci*. 2015;**133**:77–92.
37. Perschbacher KJ, Deng G, Fisher RA, Gibson-Corley KN, Santillan MK, Grobe JL. Regulators of G-protein signaling in cardiovascular function during pregnancy. *Physiol Genomics*. 2018;**50**(8):590–604.
38. Oliveira-Dos-Santos AJ, Matsumoto G, Snow BE, et al. Regulation of T cell activation, anxiety, and male aggression by RGS2. *Proc Natl Acad Sci USA*. 2000;**97**(22):12272–12277.
39. Cho H, Park C, Hwang IY, et al. Rgs5 targeting leads to chronic low blood pressure and a lean body habitus. *Mol Cell Biol*. 2008;**28**(8):2590–2597.
40. Dahlen SA, Bernadyn TF, Dixon AJ, et al. Dual loss of regulator of G protein signaling 2 and 5 exacerbates ventricular myocyte arrhythmias and disrupts the fine-tuning of $G_{i/o}$ signaling. *J Mol Cell Cardiol*. 2022;**170**:34–46.
41. Hartley CJ, Reddy AK, Madala S, Entman ML, Michael LH, Taffet GE. Doppler velocity measurements from large and small arteries of mice. *Am J Physiol Heart Circ Physiol*. 2011;**301**(2):H269–H278.
42. Sweazea KL, Walker BR. Impaired myogenic tone in mesenteric arteries from overweight rats. *Nutr Metab (Lond)*. 2012;**9**(1):18.
43. Osei-Owusu P, Collyer E, Dahlen SA, Adams RE, Tom VJ. Maladaptation of renal hemodynamics contributes to kidney dysfunction resulting from thoracic spinal cord injury in mice. *Am J Physiol Ren Physiol*. 2022;**323**(2): F120–F140.
44. Jackson WF. KV channels and the regulation of vascular smooth muscle tone. *Microcirculation*. 2018;**25**(1): e12421.
45. Roberts OL, Kamishima T, Barrett-Jolley R, Quayle JM, Dart C. Exchange protein activated by cAMP (Epac) induces vascular relaxation by activating Ca^{2+}-sensitive K+ channels in rat mesenteric artery. *J Physiol*. 2013;**591**(20):5107–5123.
46. Anand-Srivastava MB. Enhanced expression of inhibitory guanine nucleotide regulatory protein in spontaneously hypertensive rats. Relationship to adenylate cyclase inhibition. *Biochem J*. 1992;**288**(Pt 1):79–85.
47. Taussig R, Iniguez-Lluhi JA, Gilman AG. Inhibition of adenylyl cyclase by Gi alpha. *Science*. 1993;**261**(5118):218–221.
48. Siderovski DP, Willard FS. The GAPs, GEFs, and GDIs of heterotrimeric G-protein alpha subunits. *Int J Biol Sci*. 2005;**1(2)**:51–66.
49. Heximer SP, Srinivasa SP, Bernstein LS, et al. G protein selectivity is a determinant of RGS2 function. *J Biol Chem*. 1999;**274**(48):34253–34259.
50. Garcia-Morales V, Cuinas A, Elies J, Campos-Toimil M. PKA and Epac activation mediates cAMP-induced vasorelaxation by increasing endothelial NO production. *Vascul Pharmacol*. 2014;**60**(3):95–101.
51. Ferrier GR, Howlett SE. Differential effects of phosphodiesterase-sensitive and -resistant analogs of cAMP on initiation of contraction in cardiac ventricular myocytes. *J Pharmacol Exp Ther*. 2003;**306**(1):166–178.
52. Choi YJ, Lee HK, Kim SK. Doppler ultrasound investigation of female infertility. *Obstet Gynecol Sci*. 2023;**66(2)**:58–68.
53. Sher G, Fisch JD. Effect of vaginal sildenafil on the outcome of in vitro fertilization (IVF) after multiple IVF failures attributed to poor endometrial development. *Fertil Steril*. 2002;**78**(5):1073–1076.
54. Schulman H, Fleischer A, Farmakides G, Bracero L, Rochelson B, Grunfeld L. Development of uterine artery compliance

in pregnancy as detected by Doppler ultrasound. *Am J Obstet Gynecol*. 1986;**155**(5):1031–1036.
55. Cacciatore B, Simberg N, Fusaro P, Tiitinen A. Transvaginal Doppler study of uterine artery blood flow in in vitro fertilization-embryo transfer cycles. *Fertil Steril*. 1996;**66**(1):130–134.
56. Despot A, Bukovic D, Rubala D, Votava-Raic A. Transvaginal color flow imaging of the uterine artery during fertile period and postmenopause. *Coll Antropol*. 1997;**21**: 525–530.
57. Osei-Owusu P, Sabharwal R, Kaltenbronn KM, et al. Regulator of G protein signaling 2 deficiency causes endothelial dysfunction and impaired endothelium-derived hyperpolarizing factor-mediated relaxation by dysregulating $G_{i/o}$ signaling. *J Biol Chem*. 2012;**287**(15):12541–12549.
58. Holobotovskyy V, Manzur M, Tare M, et al. Regulator of G-protein signaling 5 controls blood pressure homeostasis and vessel wall remodeling. *Circ Res*. 2013;**112**(5): 781–791.
59. Tang KM, Wang GR, Lu P, et al. Regulator of G-protein signaling-2 mediates vascular smooth muscle relaxation and blood pressure. *Nat Med*. 2003;**9**(12):1506–1512.
60. Snabaitis AK, Muntendorf A, Wieland T, Avkiran M. Regulation of the extracellular signal-regulated kinase pathway in adult myocardium: differential roles of G(q/11), G(i) and G(12/13) proteins in signalling by alpha1-adrenergic, endothelin-1 and thrombin-sensitive protease-activated receptors. *Cell Signal*. 2005;**17**(5):655–664.
61. Gu S, Tirgari S, Heximer SP. The RGS2 gene product from a candidate hypertension allele shows decreased plasma membrane association and inhibition of G_q. *Mol Pharmacol*. 2008;**73**(4):1037–1043.
62. Garzon J, Rodriguez-Munoz M, de la Torre-Madrid E, Sanchez-Blazquez P. Effector antagonism by the regulators of G protein signalling (RGS) proteins causes desensitization of mu-opioid receptors in the CNS. *Psychopharmacology (Berl)*. 2005;**180**(1):1–11.
63. Riddle EL, Schwartzman RA, Bond M, Insel PA. Multi-tasking RGS proteins in the heart: the next therapeutic target? *Circ Res*. 2005;**96**(4):401–411.
64. Heximer SP, Blumer KJ. RGS proteins: swiss army knives in seven-transmembrane domain receptor signaling networks. *Sci STKE*. 2007;**2007**(370):pe2.
65. Deng Y, Dickey JE, Saito K, et al. Elucidating the role of Rgs2 expression in the PVN for metabolic homeostasis in mice. *Mol Metab*. 2022;**66**:101622.
66. Ingi T, Aoki Y. Expression of RGS2, RGS4 and RGS7 in the developing postnatal brain. *Eur J Neurosci*. 2002;**15**(5):929–936.
67. Francelle L, Galvan L, Brouillet E. Possible involvement of self-defense mechanisms in the preferential vulnerability of the striatum in Huntington's disease. *Front Cell Neurosci*. 2014;**8**:295.
68. Heximer SP. RGS2-mediated regulation of Gqalpha. *Methods Enzymol*. 2004;**390**:65–82.
69. Kehmeier MN, Bedell BR, Cullen AE, et al. In vivo arterial stiffness, but not isolated artery endothelial function, varies with the mouse estrous cycle. *Am J Physiol Heart Circ Physiol* 2022;**323**(6):H1057–H1067.
70. Karppanen T, Kaartokallio T, Klemetti MM, et al. An RGS2 3'UTR polymorphism is associated with preeclampsia in overweight women. *BMC Genet*. 2016;**17**(1):121.
71. Kvehaugen AS, Melien O, Holmen OL, Laivuori H, Dechend R, Staff AC. Hypertension after preeclampsia and relation to the C1114G polymorphism (rs4606) in *RGS2*: data from the Norwegian HUNT2 study. *BMC Med Genet*. 2014;**15**(1):28.
72. Kvehaugen AS, Melien O, Holmen OL, et al. Single nucleotide polymorphisms in G protein signaling pathway genes in preeclampsia. *Hypertension*. 2013;**61**(3):655–661.
73. Perschbacher KJ, Deng G, Sandgren JA, et al. Reduced mRNA expression of RGS2 (regulator of G protein signaling-2) in the placenta is associated with human preeclampsia and sufficient to cause features of the disorder in mice. *Hypertension*. 2020;**75**(2):569–579.

Submitted: 6 November 2023; **Revised:** 9 January 2024; **Accepted:** 16 January 2024